

Predictive modelling of H-mode and steady-state scenarios in FAST

B.Baiocchi^{1,2}, G.Calabro³, L.Lauro-Taroni^{4,5}, P.Mantica¹, A.Cardinali³, G.Corrigan⁶, F.Crisanti³, D.Farina¹, L.Figini¹, G.Giruzzi⁷, T.Johnson⁸, M.Marinucci³, V.Parail⁶

¹*Istituto di Fisica del Plasma, Euratom-ENEA-CNR Association, Milan, Italy*

²*Università degli Studi di Milano, Dipartimento di Fisica, Milan, Italy*

³*Associazione Euratom-ENEA sulla Fusione, C.P. 65-I-00044-Frascati, Rome, Italy*

⁴*New College, Oxford OX1 3BN, UK*

⁵*Consorzio RFX, ENEA-Euratom Association, Padua, Italy*

⁶*Euratom/CCFE Association, Culham Science Centre, Abingdon, OX14 3DB, UK*

⁷*Association Euratom-CEA, CEA, IRFM, F-13108 Saint Paul Lez Durance, France*

⁸*Association EURATOM-VR, Fusion Plasma Physics, EES, KTH, Stockholm, Sweden*

The Fusion Advanced Study Torus (FAST) has been proposed as a possible European ITER satellite [1] providing plasma conditions for integrated studies of plasma–wall interaction, burning plasma physics, ITER relevant operational issues and steady-state scenarios. Predicting performance and scenarios in future fusion devices beyond the level of 0D scaling laws is a challenging task. On one hand we do not yet have at disposal fully validated core and edge predictive transport models, on the other hand assuming 1D profile conservation starting from data in existing machines and using dimensionless parameter scaling is at least partially hindered by expected differences between present and future machines, such as in plasma rotation, amount of electron heating and impurity concentrations. In this situation, the predictive activity must wisely combine both theory based simulations and empirically based considerations, with the strongest possible link to experimental results in existing devices.

In this spirit, the initial study of FAST scenarios [2] has been refined by considering both the predictions of several physics based or semi-empirical transport models and the recent transport experimental results on devices such as JET, DIII-D and C-MOD. H-mode and Advanced Tokamak are the investigated FAST scenarios. For H-mode the first analyzed case is characterized by $B_t=7.5$ T and $I_p=6.5$ MA. Heating power equal to 30 MW is provided by the ICRH system at 73 MHz in (³He)-D minority scheme. $B_t=6$ T and $I_p=5.5$ MA characterize the second case, where the heating power is given by 15 MW, provided by the ICRH system at 58 MHz in (³He)-D minority, and 15 MW, provided by the ECRH system (170 GHz, 2nd Harmonic O-mode from LFS). For the Advanced Tokamak scenario $B_t=3.5$ T and $I_p=2$ MA are the chosen parameters. The heating power is 30 MW, provided by the ICRH system at 35 MHz in (³He)-D minority, and 4 MW, provided by the LH at 5 GHz, $n\parallel=2.3$.

The simulations have been carried out using the JETTO code ([3], part of the JAMS JET suite of integrated codes). For ICRH heating profiles we have either used the PION code [4]

called self-consistently by JETTO or the TORIC code [5] which is run outside JETTO and requires a few iterations. Good match between the RF deposition predicted by the two codes is shown in Fig. 1 for the case with $n_{3He}/n_e=3\%$.

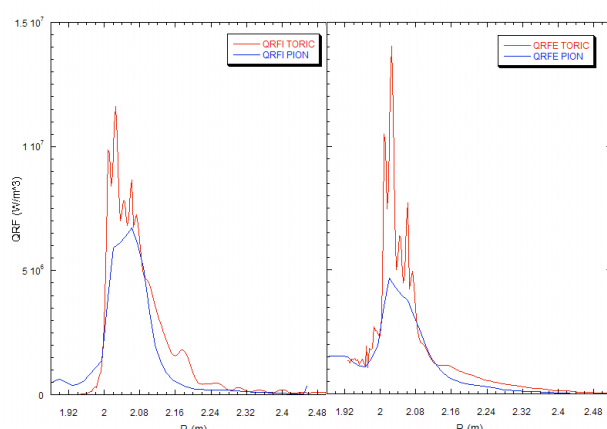


Fig. 1: ICRH deposition profiles for ions (a) and electrons (b) with red lines for TORIC and blue lines for PION (7.5T, 73 MHz, $n_{3He}/n_e=3\%$).

The ECRH heating profiles have been provided by the GRAY code [6], which is also outside the JAMS suite and required iterations with JETTO. For AT scenarios FRTC [7], within the JAMS suite, has been used to calculate LH heating and current drive profiles.

Different core transport models have been used: first principle models (Weiland [8] and GLF23 [9]) and semi-empirical models (mixed Bohm-gyroBohm (BgB) [10] and Critical Gradient Model [11]). In the CGM simulations electron threshold has been calculated after [8] and ion threshold after [12] whilst the stiffness coefficients have been chosen following the results of recent transport experiments on JET [13,14], i.e. $\chi_{se} \sim 1$ for electrons and $\chi_{si} \sim 2-4$ for ions, which implies rather high stiffness for both heat transport channels. The pedestal values have been chosen in accordance with pedestal scaling as the modelling work has focused on the core transport issues. All the simulations have been made with evolving current, ion and electron temperatures. For the H-mode scenario the density profile has been in first instance assigned with rather flat shape according to typical H-mode density profiles, in second instance calculated with first-principle models, resulting in significant peaking due to the low collisionality. In Fig. 2 the ion and electron temperature profiles together with the assigned density profile for 30 MW ICRH H-mode are shown using different transport models.

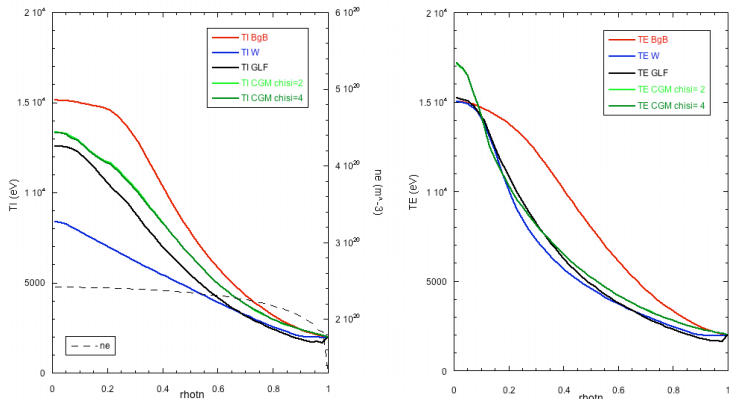


Fig. 2 Ion (a) and electron (b) temperature profiles for 7.5 T reference H-mode scenario, 30 MW ICRH calculated with PION, using different transport models: red profiles are for BgB, blue for Weiland, black for GLF 23 and green for CGM. The assigned density profile is shown in (a) with dotted line.

It is evident from Fig. 2 that, whilst for electrons the range of predicted temperatures is not large, although the BgB model gives much broader T_e profiles than all other models, for ions there is a wide range of predictions, up to a factor 2 in central T_i . A choice must then be made amongst the different models to select the most reliable prediction, since it is not granted that all the above models work well in the domain of high B_T machines, as they have commonly been validated against data of medium-size, lower B_T machines. We tend to attach better reliability to the predictions of GLF23 which has the broadest physics basis and to CGM which is derived directly from JET experimental data, and which turns out to agree to good extent with GLF23. Therefore we would retain as most reliable prediction, for the FAST reference H-mode scenario with 30 MW ICRH, values of $T_{i0} \sim 13$ keV, $T_{e0} \sim 15$ keV with a density $n_{e0} \sim 2.4 \cdot 10^{20} \text{ m}^{-3}$ and a confinement time $\tau \sim 0.4$ s, yielding $n_{e0} T_{i0} \tau \sim 1.5 \cdot 10^{21} \text{ keVs/m}^3$.

Substituting 15 MW of ICRH with 15 MW of ECRH power gives the temperature profiles shown in Fig. 3, where they are directly compared to those with 30 MW ICRH. Differently from Fig. 2, for both cases ICRH profiles are provided by TORIC, and the BgB model was used in an older version. The substitution of 15 MW ICRH with 15 MW ECRH is not beneficial from the point of view of confinement, although it alleviates the issue of high impurity influx from ICRH antenna. In fact, increased electron heating and decreased ion heating, together with the decrease in ITG threshold associated to higher T_e/T_i values and the high electron stiffness, yield colder ions and not significantly hotter electrons than the full ICRH case. Therefore we have proceeded with the analysis focusing on the 30 MW ICRH H-mode.

In order to obtain a more physics based simulation, also the density profile has been calculated consistently by the different models (BgB, Weiland, GLF23). Temperature and density profiles obtained using different transport models are shown in Fig.4. Good agreement

between the 3 different models has been found in predicting a rather peaked n_e profile, which makes conditions easier from the point of view of plasma-wall interaction, still retaining high central n_e values. The simulations with GLF23 corresponds to $T_{i0} \sim 11$ keV, $T_{e0} \sim 13$ keV with a density $n_{e0} \sim 3.3 \cdot 10^{20} \text{ m}^{-3}$ and a confinement time $\tau \sim 0.5$ s, yielding $n_{e0} T_{i0} \tau \sim 1.7 \cdot 10^{21} \text{ keVs/m}^3$.

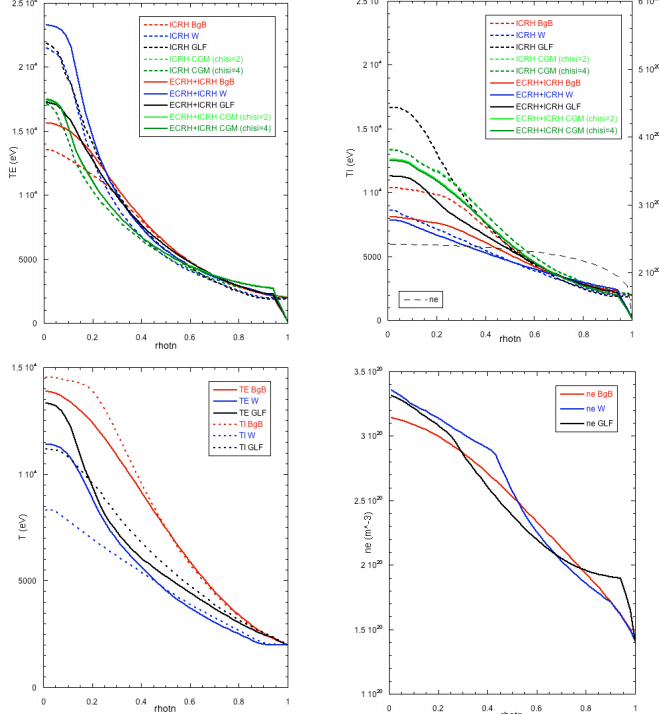


Fig.3: Ion and electron temperature and assigned density profiles for the case of 6 T H-mode with ICRH + ECRH (full line) and full ICRH (dotted line). Red lines are for old BgB, blue for Weiland, black for GLF23 and green for CGM. ICRH is calculated with TORIC.

Finally, also the role of toroidal rotation has been taken into account. From recent experimental results it seems to have a key role in achieving improved ion core confinement [13,14,15,16], not only through the well-known threshold up-shift, but through a significant reduction of the ion stiffness. Such ion core confinement improvement is an essential ingredient for obtaining steady-state scenarios with a core region of enhanced pressure gradient and associated bootstrap current. The rotation has been included in the simulations by self-consistently modelling also the momentum transport with physical assumptions consistent with recent theoretical developments [17], i.e. comparable ion heat and momentum diffusivity and an inward momentum pinch, as experimentally confirmed by several machines [e.g. 18,19]. Due to the inward pinch, core rotation in FAST can be driven by intrinsic rotation edge sources. Given the present lack of understanding and theory-based predictive capability on intrinsic rotation, we have assumed for FAST an edge rotation value $\omega_\varphi = 30$ krad/s, as provided by the scaling in [20], although such scaling has recently been questioned on the basis of new JET experimental evidence [21]. However, since high values of intrinsic rotation are measured in C-MOD, a high field compact machine conceptually similar to FAST, it may be still legitimate to assume for FAST an edge rotation value as predicted by the existing C-MOD driven empirical scaling. The simulation has been done predicting the intrinsic toroidal rotation profile using the theory indication (experimentally confirmed on JET [18, 22]) that $Pr=1$ and $Rv_\varphi / \chi_\varphi \sim 4$. No torque sources are included. Fig.5a shows the rotation profile obtained with the assumptions described above. A very significant rotation gradient is predicted. In order to estimate the rotation impact on confinement we have not used first-principle models like Weiland or GLF23, which contain only the effect on threshold, but we have used the CGM model in which the stiffness value has been decreased in the centre as found in JET and discussed in [14]. Obviously this extrapolation is totally arbitrary, but we presently lack a theoretical model describing the effect of rotation on ion stiffness, which has been experimentally found much more significant than the threshold up-shift in JET. Fig.5b

Fig. 4: Ion and electron temperature profiles (a) and calculated density profiles (b) for 7.5 T reference H-mode scenario, 30 MW ICRH calculated with PION, using different transport models: Bohm-gyroBohm in red, Weiland in blue, GLF23 in black.

shows the impact on ions (electrons are unaffected by rotation). It is seen that in this H-mode scenario, given the small volume in which ion stiffness is reduced, the impact of rotation is not large. The role of rotation is however essential in AT scenarios, as it has been shown experimentally in several machines that q profile alone is not sufficient to provide ion ITB formation. A test simulation of an AT scenario with reversed q and with/without rotation using the BgB model is shown in Fig.6. One can see that rotation helps in producing an ITB formation. A fully non-inductive pulse can be achieved with the intrinsic edge rotation, fully reversed q profile, and sustained ITB at $\rho \sim 0.3-0.4$. Indicative values are $T_{i0} \sim 12$ keV, $T_{e0} \sim 10$ keV with a density $n_{e0} \sim 2 \cdot 10^{20} \text{ m}^{-3}$ and a confinement time $\tau \sim 0.1$ s, yielding a value $n_{e0} T_{i0} \tau \sim 2.4 \cdot 10^{20} \text{ keVs/m}^3$. More simulations of AT scenarios using physics based models and CGM are planned in the near future, including also the possibility of 10 MW NNBI power as described in [23], providing a sounder source of rotation than just the intrinsic one.

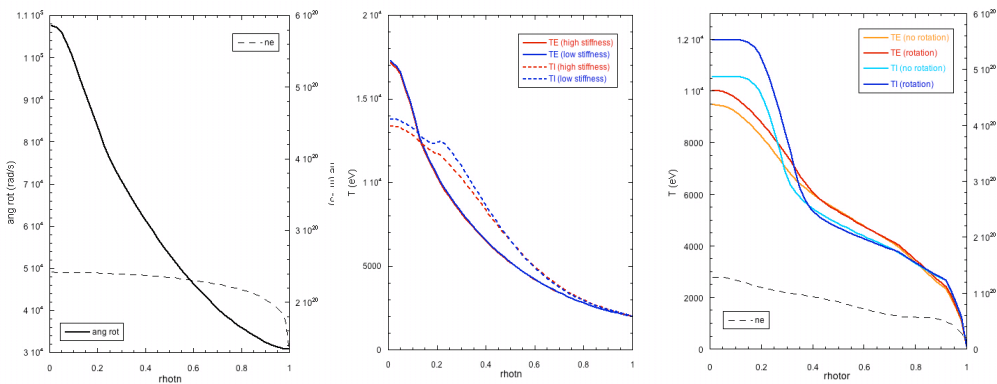


Fig. 5: Assigned density and calculated rotation (a) and T_i , T_e (b) profiles for 7.5 T 30 MW ICRH H-mode scenario using $Pr=1$, $Rv_\phi/\chi_\phi \sim 4$ and edge intrinsic rotation for momentum transport and CGM for heat transport with low ion stiffness in the rotating case.

Fig. 6: Ion and electron temperature and density profiles without and with rotation for a 3.5 T ICRH+LH AT scenario with reversed q profile. Rotation is driven by edge intrinsic rotation

and momentum pinch. Bohm-gyroBohm is used for heat transport and TORIC for ICRH.

In conclusions, refined transport modelling of FAST scenarios based on a careful combination of existing theory based models and latest experimental results from existing machines confirmed the expectation that FAST will be a valuable aid to ITER exploitation and provided scenario simulations on which fast particle and burning plasma studies can be performed.

This work, supported by the European Communities under the contract of Association EURATOM/ ENEA-CNR, was carried out within the framework of EFDA. The views and opinions expressed herein do not necessarily reflect those of the European Commission.

References

- [1] A.Cardinali et al., Nucl. Fusion **49** 095020 (2009)
- [2] G.Calabò et al., Nucl. Fusion **49** 055002 (2009)
- [3] G.Cenacchi and A.Taroni 1988, *JETTO: A free boundary plasma transport code (basic version)* Rapporto ENEA RT/TIB 1988(5).
- [4] L-G Eriksson et al Nucl. Fusion **33** 1037 (1993)
- [5] M.Brambilla, Plasma Phys.Contr.Fusion **41** (1999)1
- [6] Farina D. 2005 GRAY: a quasi-optical ray tracing code for electron cyclotron absorption and current drive in tokamaks *IFP-CNR Internal Report FP 05/1* and <http://www.ifp.cnr.it/publications/2005/FP05-01.pdf>
- [7] Esterkin A.R. and Piliya A.D. 1996 Nucl. Fusion **36** 1501
- [8] J.Weiland, *Collective Modes in Inhomogeneous Plasmas*, IOP (2000)
- [9] R E Waltz et al, Phys. Plasmas **4** (1997) 2482
- [10] M. Erba , A Cherubini , V V Parail , E Springmann and A Taroni , Plasma Phys. Control. Fusion **39**, 261 (1997)
- [11] X.Garbet et al., Plasma Phys. Contr. Fusion **46** (2004) 135
- [12] Romanelli, Phys. Fluids B **1**, 1018 (1989)
- [13] P.Mantica et al., Fusion Science and Technology **53** 1152 (2008)
- [14] P.Mantica et al., Phys. Rev. Lett. **102** 175002 (2009)
- [15] P.De Vries et al., Nucl. Fusion **49** 075007 (2009)
- [16] P.A.Politzer et al., Nucl. Fusion **48** 075001 (2008)
- [17] A.Peeters et al., Phys. Rev. Lett. **98** 265003 (2007)
- [18] T.Tala et al., Phys. Rev. Lett. **102** 075001 (2009)
- [19] W.M.Solomon et al., Nucl. Fusion **49** 085005 (2009)
- [20] J.Rice et al., Nucl. Fusion **47** 1618 (2007)
- [22] P.Mantica et al., submitted to Phys. Plasmas
- [21] F.Nave et al., this conference
- [23] M.Baruzzo et al., this conference